Fermi National Accelerator Laboratory

FERMILAB-Conf-94/325-E

Charmonium Production, b Quark and B Meson Production and $b\ \bar{b}$ Correlations at CDF

K. Byrum

Fermi National Accelerator Laboratory
P.O. Box 500, Batavia, Illinois 60510

Argonne National Laboratory,
Argonne, Illinois, 60439

September 1994

Published Proceedings *27th International Conference on High Energy Physics, University of Glasgow,* Glasgow, Scotland, July 20-27, 1994

Disclaimer

CDF/PUB/BOTTOM/PUBLIC/2822
FERMILAB-CONF-94/325-E

Published Proceedings 27th International Conference on High Energy Physics, University of Glasgow, Glasgow, Scotland, July 20-27, 1994.

Charmonium Production, b Quark and B Meson Production and $b\bar{b}$ Correlations at CDF

K. Byrum[†‡]

† Argonne National Laboratory, Argonne, Illinois 60439 USA

Abstract

We present results on charmonium production, b quark and B meson production and $B\bar{B}$ correlations using data taken with the CDF detector at Fermilab in $p\bar{p}$ collisions at $\sqrt{s} = 1.8$TEV during the 1992-93 collider run.

1. Introduction

Understanding the production processes of heavy quarks in high energy hadronic collisions is fundamental for testing the theory of perturbative QCD in the next to leading order (NLO) calculation. Calculations of the b quark and B meson production cross sections at NLO have been performed by many authors [1,2,3,4,5,6] and are predicted to have large uncertainties due to choices in the renormalization scale μ, the b quark mass and the partonic distribution functions. While earlier UA1 results [7,8] were at reasonable agreement with NLO QCD calculations at $\sqrt{s} = 630$GeV, the 1989 CDF results tended to be roughly a factor of two higher than the theoretical central values [9]. In this paper, we use the 1992-93 data to refine our earlier cross section measurements.

We begin with a discussion of the CDF detector components relevant for the results shown here and also briefly describe the triggers used to collect this data. We start our physics discussion with a description of the theory of charmonium production and present measurements of the inclusive J/ψ and $\psi(2s)$ differential cross sections. We next present differential B meson cross sections using fully reconstructed $B^{\pm} \rightarrow J/\psi K^{\pm}$ and $B^0 \rightarrow J/\psi K^{*0}$ events and partially reconstructed $\bar{B} \rightarrow D^0\mu^- X$ events. We next present the b quark cross section using some of the above channels along with the inclusive $B \rightarrow \mu^- X$ channel. Finally, we conclude with results that study the correlated $b\bar{b}$ cross section as a function of the azimuthal angle between the b and $\bar{b}$. In this paper, reference to any particular state implies the charge conjugate state as well.

‡ E-mail: byrum@fnald.fnal.gov.

1.1. *Detector Description*

The CDF detector is described in detail elsewhere [10]. We describe here only those components relevant for the results presented. The CDF coordinate system defines the beam line to be the z direction. R is the radial distance from the beam line and ϕ is the azimuthal angle.

Two tracking systems inside a 1.4T solenoidal magnetic field provide the $R-\phi$ momentum analysis for charged particles. The Silicon Vertex Detector (SVX) [11] is a four layer silicon microstrip device with a radii ranging from 3 to 8cm and covering the luminous region of $|z|$ <26cm. The hit resolution is 13 μm and the impact parameter resolution is $(13 + 40/p_T)\mu$m. The rms size of the beam spot is 35μm so that not all events at CDF have vertices within the fiducial volume of the SVX. The Central Tracking Chamber (CTC) [12] is an 84-layer cylindrical drift chamber with radii ranging from 309 to 1320cm and covers the pseudorapidity range of $|\eta|$ <1.1. The momentum resolution for the CTC alone is $\Delta p_T/p_T$=.0066+.0014p_T and for the combined SVX-CTC system is $\Delta p_T/p_T$=.0066+.0009p_T

Outside the solenoid are the central electromagnetic

(CEM) and hadronic (CHA) calorimeters which provide five absorption lengths of material before the Central Muon Chambers (CMU). The CMU is a four-layer "limited streamer" chamber covering 85% of the azimuthal region for $|\eta| < 0.6$. Muons with p_T below $\approx$1.4 GeV/c range out in the calorimeters. Behind the CMU system are three absorption lengths of steel followed by the Central Muon Upgrade chambers (CMP). The CMP is a four-layer drift chamber covering 53% of the azimuthal region for $|\eta| < 0.6$. Both of these chambers reconstruct short tracks of up to four hits called "stubs".

1.2. Triggers

The CDF trigger [13] consists of three levels. For discussions in this paper, I will describe only the muon b triggers. In the first level of triggering (L1), we require one central muon stub with $p_T > 6$GeV/c for the inclusive muon trigger and two or more central muon stubs with $p_T > 3$GeV/c for the dimuon trigger. At the second level of triggering (L2), the Central Fast Tracker (CFT) [14] is run. The CFT is a hardware track finder with a transverse momentum resolution of $\Delta p_T/p_T^2 = 3.5\%$. The L2 tracks are matched to the muon L1 stubs to within 5°. The inclusive muon events require CFT tracks with $p_T > 9.2$GeV/c. The dimuon events require one stub have a matching CFT track with $p_T > 3$GeV/c. The third level of triggering (L3) [15,16] consists of a 1000 MIP microprocessor farm from which the offline reconstruction software is run. The L3 thresholds for the muons are matched to their L2 values.

2. Charmonium Production

The theory of charmonium production in hadronic collisions has been studied within the perturbative QCD model for quite awhile [17,18,19,20,21,22]. At the energies of the Tevatron, the production of J/ψ and $\psi(2s)$ is expected to be dominated by the lowest order two to two subprocesses [6]. Direct charmonium production is described by the processes $gg, q\bar{q}, gq \rightarrow \chi g$ followed by the decay $\chi \rightarrow J/\psi, \gamma$ Production through the decay of a B meson is described by the processes $gg, q\bar{q} \rightarrow b\bar{b}$ and $gq \rightarrow b\bar{b}g$ followed by the decay $b \rightarrow \bar{B} \rightarrow J/\psi X$. Only at $O(\alpha^3)$ can the J/ψ and $\psi(2s)$ be produced directly due to spin parity conservation.

If one assumes this theoretical description, J/ψ production should be dominated by χ and B production while the $\psi(2s)$ production should be dominated by B production. More recently, it has been suggested that there exist a class of higher order processes which are less suppressed than the leading order ones at large p_T [23,24,25]. These higher order processes can contribute to charmonium production when a high p_T gluon or charm quark fragments into charmonium states.

Studies of the charmonium production at CDF produce our lowest p_T b cross section measurements. In our earlier measurements [26], we relied on the theoretical assumption described above to measure f_b, the fraction of inclusive J/ψ and $\psi(2s)$ events from B decays. With the addition of the SVX, we are now able to measure secondary vertices and separate those J/ψ and $\psi(2s)$ events produced via prompt charmonium production from those events produced from B decays in a model independent way [27].

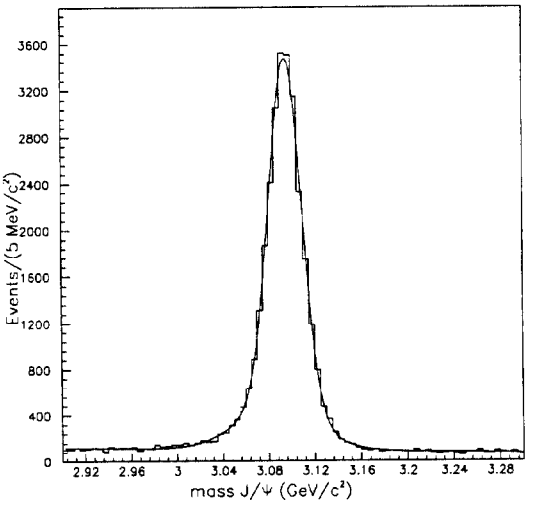

Figure 1. The J/ψ Invariant Mass distribution.

We reconstruct our J/ψ and $\psi(2s)$ events through the decay to muons and require the muons pass all three levels of trigger. We also require $p_T^{\psi,\psi(2s)} > 4$GeV/c and $|\eta^{\psi,\psi(2s)}| < .6$ and the invariant mass of the dimuon pair be within 50 MeV of the world $J/\psi, \psi(2s)$ average. Figure 1 shows the invariant mass distribution for the J/ψ events. Figure 2 shows the pseudo $c\tau$ lifetime distribution for the inclusive $\psi(2s)$ where $c\tau = L_{xy} * M_B/(p_T * F^c)$. L_{xy} is the projection of the decay length onto the $J/\psi, \psi(2s)$ transverse momentum and F^c is a Monte Carlo correction factor that relates the $J/\psi, \psi(2s)$ transverse momentum to the transverse momentum of the parent. Events in figure 2 are further required to have both muons be reconstructed as good quality SVX tracks. The B fraction is determined from a fit over this distribution.

Figure 3 shows the differential J/ψ cross section as a function of the $p_T(J/\psi)$ for $|\eta| <.6$ and $J/\psi \rightarrow$

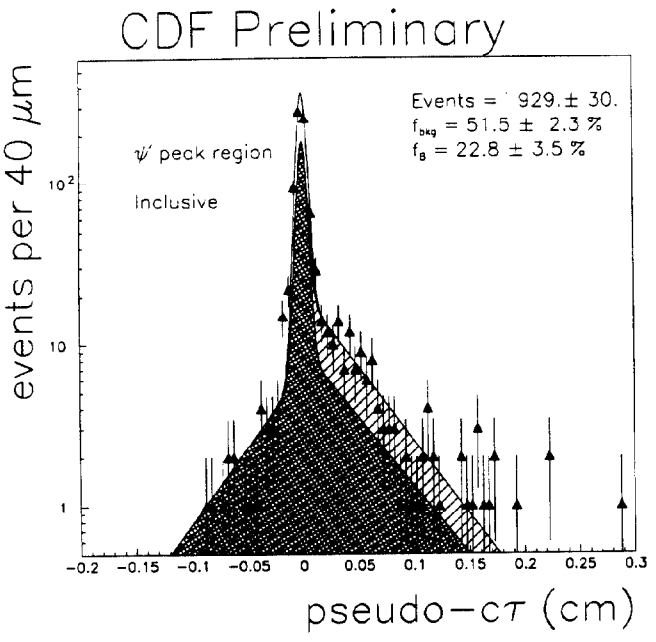

Figure 2. The $\psi(2s)$ Lifetime Pseudo $c\tau$ distribution. The dark region is the background shape and the slashed region is the B component, plus the background shape. The clear region shows an excess of prompt events.

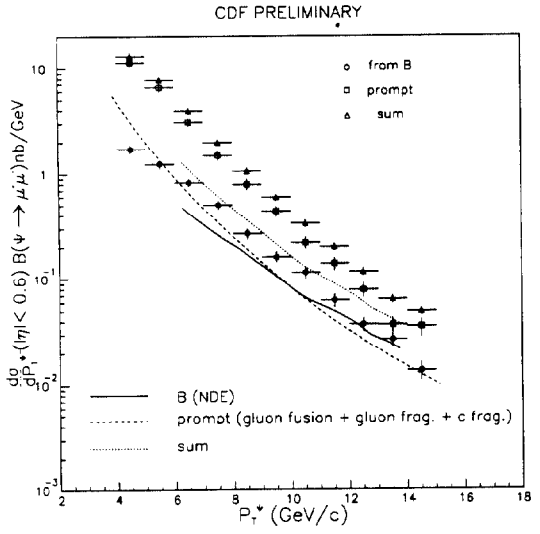

Figure 3. $d\sigma/dp_T(|\eta| < .6)J/\psi \rightarrow \mu\mu$ (nb/GeV).

$\mu\mu$. Three sets of data points are shown, the prompt component, the component from B decays and the total. The data points are each compared to theory curves. The excess over the predicted total cross section is primarily due to the prompt component. Even though the contribution from gluon fragmentation [23,24,25] has been included in the theory curves, the prompt theory still does not adequately describe the data.

The NLO theory curves [1] for the B component use MRSD0 structure functions with a renormalization scale of $\mu = \mu_0 = \sqrt{M_b^2 + p_T^2}$. The measured values are roughly a factor of two higher than the theoretical predictions. With a choice of the renormalization scale set to $\mu = \mu_0/4$, there is better agreement between the theory curves and the measured data. Motivations for choosing different renormalization scales is a separate topic of this conference [28].

The differential cross section for the $\psi(2s)$ is shown in Figure 4. Theoretical curves are shown for the prompt component and for the B component. The predicted prompt cross section is more than an order of magnitude lower than the observed data. The B production NLO theory [1] with the renormalization scale $\mu = \mu_0$ is again roughly a factor of two lower than the $\psi(2s)$ data points.

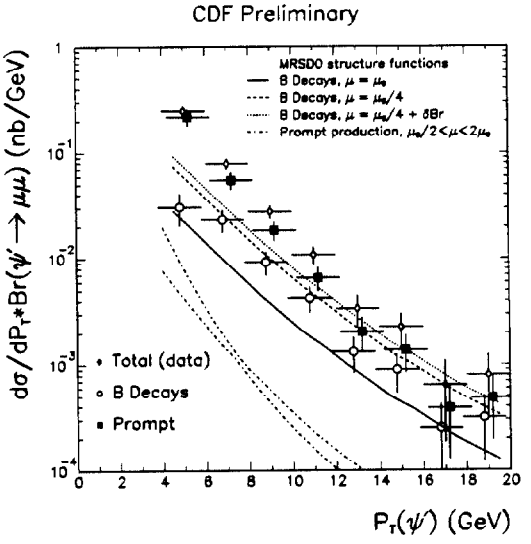

Figure 4. $d\sigma/dp_T(|\eta| < .6)J/\psi(2s) \rightarrow \mu\mu$ (nb/GeV).

The discrepancy between the data and the theory of prompt charmonium production is currently under study [29]. Higher order diagrams such as $gg \rightarrow J/\psi gg$ are being calculated and these contributions, for which

the hard-scattering cross section has a p_T dependence, are expected to be intermediate between the LO and NLO corrections. Experimentally, CDF is in the midst of Run 1b and has already accumulated approximately $20pb^{-1}$ of new data. In the coming months, we plan to extend our measurements to the Υ system and should have differential cross sections for all three triplet S states by the end of the year. Additionally, we plan to search for excited χ states from which the $\psi(2s)$ could decay through the decay chain $\chi \rightarrow \psi(2s)\gamma$ by searching for the presence of an associated photon with the $\psi(2s)$.

3. B Meson Production

We measure the differential $B^{\pm}$ and B^0 cross sections [30] as a function of the transverse momentum by fully reconstructing the B meson decays, $B^{\pm} \rightarrow J/\psi K^{\pm}$ and $B^0 \rightarrow J/\psi K^{*0}$, where the J/ψ is required to decay to two muons, and the K^{*0} is required to decay to $K^{\pm}\pi^{\mp}$. The reconstructed J/ψ is required to pass all three levels of the dimuon trigger and the invariant mass is required to be within 3σ of the J/ψ mass world average. SVX track information is used if available, otherwise CTC track information is used. Since kaons from $B^{\pm}$ decays have a harder p_T spectrum than particles from the underlying event, $p_T(K^{\pm,*0}) > 1.25$GeV/c. The B meson is required to have $p_T(B) > 6.$GeV/c. The invariant $K-\pi$ mass is required to be within 50MeV of the mass of the K^{*0} and only the combination closest to the world average K^{*0} mass of 896.1 MeV/c^2 is used to avoid double counting. A confidence level cut of $P(\chi^2) > .005$ is applied to the fit which constrains the decay tracks to come from a common vertex and requires the invariant dimuon mass to equal the J/ψ mass. There is also a cut on the proper decay length, $c\tau > 100\mu$m where $c\tau = L_{xy} * M_b/p_T$. This cut removes about 75% of the background while less than 20% of the signal is lost.

The $J/\psi K^{\pm}$ events are divided into 4 bins in p_T, 6-9,9-12,12-15 and >15 and the $J/\psi K^{*0}$ events are divided into 3 bins in p_T, 7-11,11-15 and >15. The choice of bin size leads to comparable statistical and systematic uncertainties. Only integrated cross-sections are determined for the last bins. Figure 5 shows the $B^{\pm}$ meson invariant mass distribution in the different bins of p_T.

We also measure the B cross section using the partially reconstructed decay $B \rightarrow \mu^- D^0 X$ where $D^0 \rightarrow K^-\pi^+$ and the decay $B \rightarrow \mu^- D^{*+} X$ where $D^{*+} \rightarrow D^0\pi^+$ and $D^0 \rightarrow K^-\pi^+$ [31]. The muon is required to pass all three levels of trigger with $p_T > 7.6$GeV/c. For reconstructing the D mesons, charged tracks are assigned kaon and pion masses and the invariant $K^-\pi^+$ and $K^-\pi^+\pi_b^+$ masses are computed for tracks satisfying $p_T^{K,\pi}$ >1.5GeV/c and $p_T^{K,\pi}$(Max)>3.0GeV/c. Events

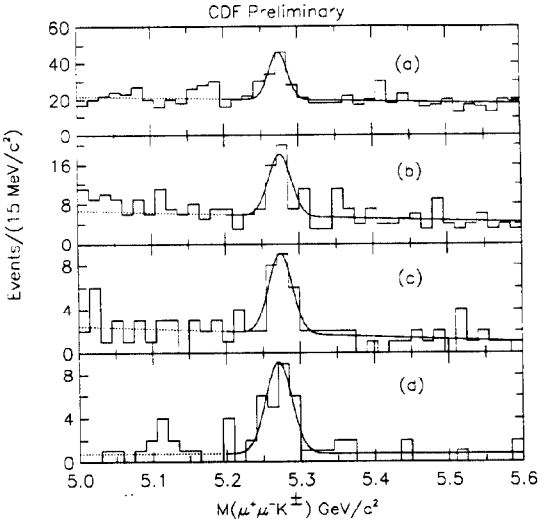

Figure 5. $B^{\pm}$ meson invariant mass distribution from the decay $B^{\pm} \rightarrow J/\psi K^{\pm}$ for the following momentum ranges: (a) 6-9 GeV/c, (b) 9-12 GeV/c, (c) 12-15 GeV/c, and (d) >15 GeV/c.

with $M(K\pi\pi) - M(K\pi) < 153$MeV are tagged as D^* candidates. For D^0 events, if the charge of the kaon matches the charge of the muon, the event is tagged as a "right-sign" combination, otherwise the event is tagged as a "wrong-sign" combination. For D^* events, "right-sign" combinations are those events where the sign of the π_b is opposite to the sign of the lepton and conversely for "wrong-sign" combinations. The invariant mass distribution of the "wrong-sign" combinations is used as a measure of the background. Figure 6 shows the invariant mass distribution for the "right-sign" and "wrong-sign" $K\pi$ combinations.

The differential cross section of the B meson is shown in Figure 7 compared to a NLO calculation [1] convoluted with Peterson fragmentation [32]. MRSD0 structure functions are used with $\mu = \mu_0 = \sqrt{M_b^2 + p_T^2}$. Not shown in this figure is a common systematic uncertainty due to the branching ratio of $\pm 24\%$ for the $J/\psi K^{*0}$ points and $\pm 15\%$ for the $J/\psi K^-$ points.

4. b Quark Production

The b quark cross section is measured using the inclusive muon channel $B \rightarrow \mu X$ by determining F_b, the fraction of muons originating from B decays [33]. F_b is determined using the muon track impact parameter

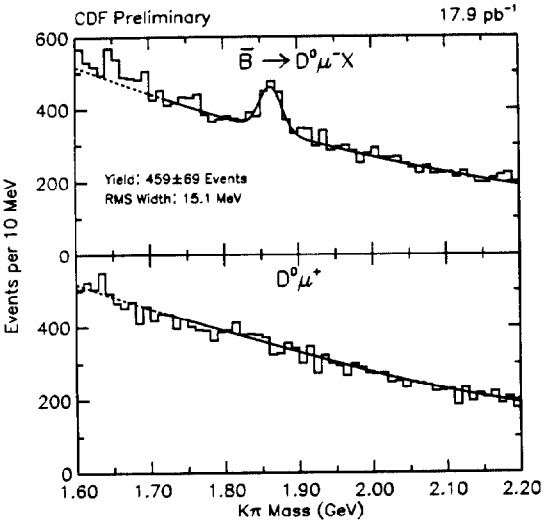

Figure 6. The invariant mass distribution for the decay D^0 from $B \to \mu D^0 X$ for a.) "right-sign" combinations and b.) "wrong-sign" $K\pi$ combinations.

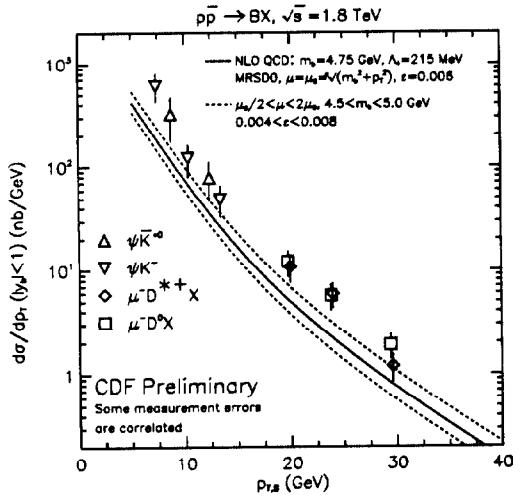

Figure 7. $d\sigma/dp_T(|\eta| < 1)(p\bar{p} \to BX)$. Not shown in this figure is a common systematic uncertainty due to the branching ratio of $\pm 24\%$ for the $J/\psi K^{*0}$ points and $\pm 15\%$ for the $J/\psi K^-$ points.

measured in the SVX. This method relies on the fact that B mesons have long lifetimes compared to the vertex resolution of the SVX detector. Using the impact parameter, it is easy to distinguish the long-lived B and C mesons from the prompt background.

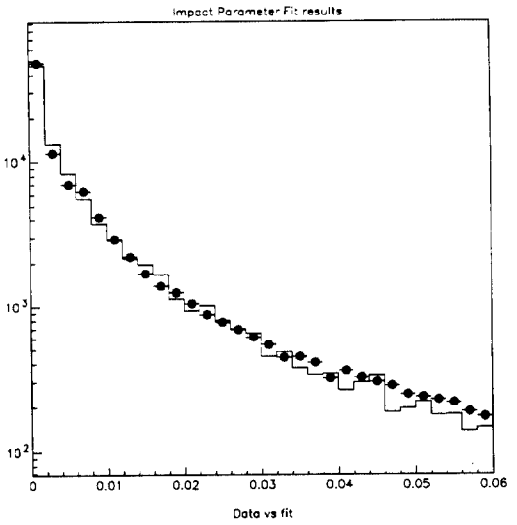

Figure 8. For 9 GeV muons, we show the impact parameter distribution (cm) overlaid with the fit results. The data are shown as the points and the boxed distribution is the sum of the input spectrums. The fraction of muons from B decays in the sample is $36 \pm 2.4\%$ where the error is statistical only.

For this measurement, good quality muons are required to pass all three levels of the trigger with $p_T > 9\text{GeV/c}$. The data is assumed to be a composition of a bottom component plus a charm component plus a background component. Monte Carlo data is used to parameterize the impact parameter distribution for the bottom and charm component and the background is parameterized using tracks from a sample of jet triggered data. Figure 8 shows the result of a binned maximum likelihood fit using the three input distributions and compared to the inclusive muon data.

The b quark cross section measurements are shown in Figure 9. The theory curves are based on the NLO calculation by Nason, Dawson and Ellis [1] convoluted with Peterson fragmentation [32]. The NLO theory uses MRSD0 structure functions, $\mu = \mu_0 = \sqrt{M_b^2 + p_T^2}$ and $M_b = 4.75\text{GeV}$. The dashed lines correspond to the upper and lower allowed predictions with variations in μ and M_b. The various data points have been derived

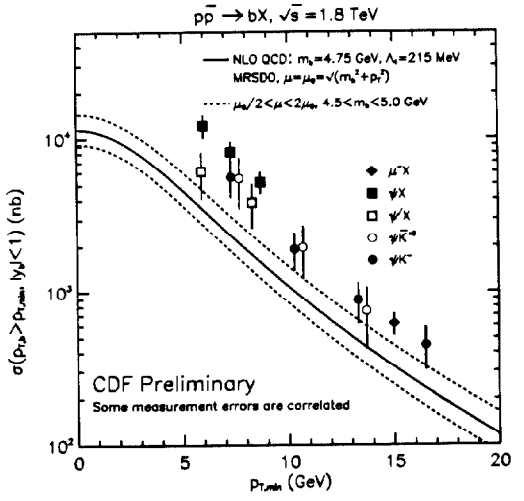

Figure 9. $\sigma(|\eta| < 1.)p\bar{p} \rightarrow bX$

by using the measured integrated cross sections (from the specific channels mentioned earlier in this text) normalized to a b quark acceptance of $p_T^b > p_T(\text{min})$ and $|y|$ <1.0. The points are plotted at the $p_T(\text{min})$ value.

As with the differential cross section distributions, the data lie approximately a factor of 2 above the central theory curve. The biggest difference between the results presented here and our earlier measurements [9] is that the J/ψ and $\psi(2s)$ points have come down. This is due to the fact that the measured f_b is smaller than the theoretical number assumed in the 1988-1989 analysis.

5. $B\bar{B}$ Correlation Studies

We also present a measurement of the correlated b quark cross section, where one b is detected from the lepton from semileptonic decay and the other b is detected with secondary vertexing techniques [34]. The secondary vertex technique [35,36] uses a prescribed algorithm requiring the presence of a jet with uncorrected E_t >10GeV/c and answers the question "Is the ensemble of tracks in a jet consistent with being from the primary vertex?". The algorithm assigns a probability between 0 and 1 to each jet which has at least two good tracks with a probability value near 1 indicating that the jet is very consistent with being primary, while a probability near 0 indicates the jet is very inconsistent with being primary.

For this measurement, good quality muons are required to pass all three levels of the trigger with p_T > 9GeV/c and the event vertex is required to be less than 30cm to select events within the SVX fiducial volume. The events are further required to have a jet with uncorrected E_t >10GeV which contains at least 2 good quality tracks. The space angle between the muon and jet is required to be greater than $\Delta R_{jt,\mu}$ > 1.0 to ensure the muon is not associated with the jet and the jet is required to be within η < 1.5. The fit method is identical to the inclusive muon analysis described in section 4. The data is described as a combination of bottom plus charm plus background and a binned maximum likelihood fit is performed on the jet probability distribution using three input distributions and the data.

Figure 10 shows the distribution of the cross section as a function of the azimuthal angle between the jet and the muon, overlaid with a theoretical prediction. The theory curve uses the Mangano-Nason-Ridolfi calculation [3] with $M_b = 4.75$, MRSB structure functions and $\mu = \mu_0$ for $|\eta^{b1}|$ < 1, p_T^{b1} >15GeV, $|\eta^{b2}|$ <1.5 and p_T^{b2} >10GeV. From this distribution, we note that the shapes of the theoretical prediction and the data agree well with each other.

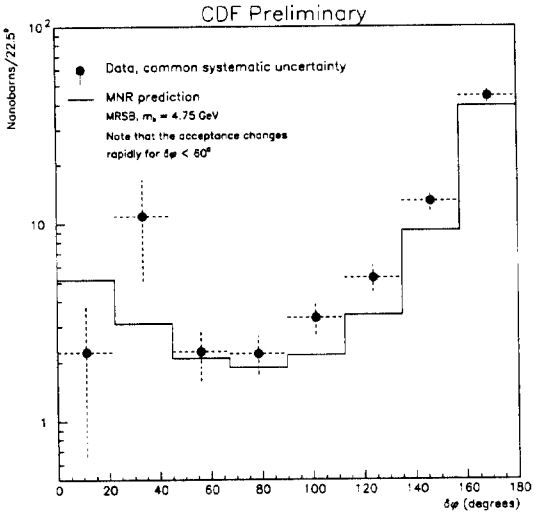

Figure 10. The distribution of the cross section as a function of the azimuthal angle between the jet and the muon, overlaid with a theoretical prediction. There is a common systematic uncertainty of +18.3 - 15.4 % not included in the experimental points.

References

[1] P.Nason,S.Dawson and R.Ellis, Nucl. Phys. **B303** (1988) 607; **B327** (1989) 49; **B335** (1990) 260.

[2] W.Beenakker,W.Van Neervan,R.Meng,G.Schuler and J.Smith, Nucl. Phys. **B351** (1991)

[3] M.Mangano,P.Nason and G.Ridolfi, Nucl. Phys. **B373** (1992) 295; **B405** (1993) 507.

[4] E.Levin,M.Ryskin,Y.Shabelski, and A.Shuvaev, DESY 91-065, (June 1991), ISSN 0418-9833.

[5] G.Altarelli,M.Diemoz,G.Martinelli, and P.Nason, Nucl. Phys. **B308** (1988) 724.

[6] E.Berger and R.Meng Argonne Preprint: ANL-HEP-PR-92-11 (1992), Phys. Rev. D Vol **49**, No. 7, (1994) 3248.

[7] M.L.Mangano, IFUP-TH (Feb. 1993)

[8] UA1 Collaboration: C.Albajar *et al.*, Phys. Lett. **256B** (1991), 121.

[9] CDF Collaboration: F. Abe *et al.*, Phys. Rev. Lett. **69** (1992) 3704, **71** (1993) 500, **71** (1993) 2537, **71** (1993) 2396, FERMILAB-PUB-93-131-E (June 1993)submitted to Phys. Rev. D.

[10] CDF Collaboration: F. Abe *et al.*, Nucl. Instr. Meth. **A271** (1988) 387.

[11] D. Amidei *et al.* Nucl. Instr. Meth. **A289** (1990) 388.

[12] F. Bedeschi *et al.* Nucl. Instr. Meth. **A268** (1988) 50.

[13] D. Amidei *et al.* Nucl. Instr. Meth. **A269** (1988) 51.

[14] G. Foster *et al.* Nucl. Instr. Meth. **A269** (1988) 93.

[15] J.Carroll *et al.* Nucl. Instr. Meth. **A300** (1991) 552.

[16] U.Joshi *et al.* Nucl. Phys. B. **23A** (1991) 365.

[17] E.Berger and D.Jones, Phys. Rev. **D23** (1981) 1521.

[18] R.Baier and R. Ruckl, Z. Phys. **C19** (1983) 251.

[19] B.Humpert, Phys. Lett. **184B** (1987) 105.

[20] R.Gastmans,W.Troost and T.Wu, Nucl. Phys. **B291** (1987) 731.

[21] E.Glover,A.Martin and W.Stirling, Z. Phys. **C38** (1988) 473

[22] E.Glover,F.Halzen and A.Martin, Phys. Lett. **185B** (1987) 441.

[23] E.Braaten and T.Yuan, Phys. Rev. Lett. **71** (1993 1673. FERMILAB-PUB-94-0400-T

[24] M. Doncheski, S.Fleming and M. Mangano, FNAL-CONF-93-348-T; FNAL-PUB-94-135-T, hep-ph-9405407.

[25] M.Cacciari and M.Greco, FNT-T-94/24, hep-ph/94405241.

[26] CDF Collaboration: F.Abe *et al.* Phys. Rev. Lett **69** (1992) 3704, **71** (1993) 2537

[27] CDF Collaboration: F.Abe *et al.* FERMILAB-Con-94-136-E.

[28] M.Mangano, to appear in the ICHEP94 proceedings, 20-27 July 1994; Glasgow, Scotland.

[29] M.Mangano, *Phenomenology of B Quark Production in Hadronic Collisions* to appear in the Proceedings of the XXIX Rencontres de Moriond, 19-26 March 1994; Meribel, France.

[30] CDF Collaboration: F.Abe *et al.* FERMILAB-Con-94-141-E.

[31] CDF Collaboration: F.Abe *et al.* FERMILAB-Con-94-134-E.

[32] C.Peterson,D.Schlatter,I.Schmitt and P.Zerwas, Phys. Rev. **D27** (1983) 105.

[33] T.Song, *et al.* CDFNOTE 2004.

[34] CDF Collaboration: F.Abe *et al.* FERMILAB-Con-94-129-E.

[35] D.Gerdes, *et al.* CDFNOTE 2023.

[36] D.Amidei, *et al.* CDFNOTE 2091.